

Influence of domain wall scattering on the magnetoresistance of Co and Co₈₀Pt₂₀ film systems

H. C. Herper and P. Entel

Physics Department, University of Duisburg-Essen, 47048 Duisburg, Germany

(Received 22 October 2007; revised manuscript received 31 March 2008; published 5 May 2008)

Constant miniaturization of electronic devices and storage media demands a detailed understanding of transport processes and structures on the atomic scale. In particular, interfaces between magnetic domains play an important role because of domain wall pinning at the interfaces. Here, we study the anisotropic magnetoresistance and the influence of domain walls on the resistance in Co and Co₈₀Pt₂₀ films in contact with Pt leads as a function of the geometry and thickness of the ferromagnetic films. The calculations were performed by using a fully relativistic *ab initio* scattering approach (Korringa–Kohn–Rostoker) and the Kubo–Greenwood formalism. In particular, the relation between the width of the domain wall and its contribution to the magnetoresistance was calculated and compared to a model calculation by Levy and Zhang [Phys. Rev. Lett. **79**, 5110 (1997)]. In the case of the current perpendicular to the plane geometry, the calculated decay of the domain wall magnetoresistance corresponds to the predicted $1/L^2$ ($L \hat{=}$ domain wall width) scaling behavior for the case of wide domain walls. For domain walls smaller than a critical width L_{\min} , a linear decay of the magnetoresistance is observed. A second type of domain walls with its magnetic orientation being partially out of plane was investigated. In this case, no $1/L^2$ behavior was found.

DOI: [10.1103/PhysRevB.77.174406](https://doi.org/10.1103/PhysRevB.77.174406)

PACS number(s): 75.47.De, 71.15.Mb, 75.60.Ch, 75.70.Cn

I. INTRODUCTION

The giant magnetoresistance (GMR) effect in systems with alternating ferromagnetic (FM) and nonmagnetic layers has been intensively studied during the last 20 years^{1–6} and is now widely used in technical devices, such as in read heads and in more future oriented magnetoresistive random access memory technology. The GMR effect originates from the dependence of the resistance on the relative orientation of the magnetic moments in two adjacent magnetic domains. Aiming for higher storage densities requires reduction of the size of the magnetic domains and, therefore, interfacial effects become more and more important. In the present paper, we consider the influence of domain walls near interfaces separating regions with different magnetic orientations.

It is known for long that domain walls will provide additional contributions to the magnetoresistance;⁷ however, measurement of the domain wall magnetoresistance (DWMR) is quite challenging. In order to avoid contributions from the anisotropic magnetoresistance (AMR), the current has to be oriented perpendicular to the magnetic moments of the domain wall. The first attempts of measuring the magnetoresistance effect of a domain wall in a single magnetic film were undertaken by Gregg *et al.*⁸ In the case of hcp(0001) Co on Al₂O₃, they observed an increase in the resistance by 0.52 $\mu\Omega$ cm (5%), which was ascribed to the presence of domain walls. Recently, direct measurements of the DWMR were performed by Prieto *et al.*,⁹ who investigated a thin Permalloy (Py)/Gd/Py system, for which in the case of antiparallel alignment of the Py layers, the magnetic moments of the Gd film form a Bloch wall. Hassel *et al.*¹⁰ measured the DWMR in polycrystalline Co-Pt wires, generating the domain walls by ion beam radiation.

Besides the dynamic properties of domain walls in thin films, which can be well described by Monte Carlo simulations,¹¹ quantum mechanical models were developed to investigate the influence of domain wall width and mobil-

ity on the electric transport, e.g., the DWMR.^{12,13} Simultaneously, *ab initio* descriptions of the DWMR based on the Green's functions techniques were developed. Early calculations of van Hoof *et al.*¹⁴ applying the Landauer formalism to transition metal films showed the importance of domain walls on the magnetoresistance. Alternatively, Yavorsky *et al.*¹⁵ investigated Bloch walls in bcc Fe by using the linearized Boltzmann equation. They observed oscillations of the GMR as a function of the domain wall width, which they ascribed to quantum well states near the Fermi level. *Ab initio* transport calculations of Gallego *et al.*¹⁶ showed the influence of Bloch walls on the AMR in Py. They investigated domain walls with the magnetization oriented parallel to the plane of layers (here, the \hat{x} - \hat{y} plane) and current in plane (CIP) (parallel to the \hat{x} direction).

Our aim is to study the DWMR of Co and Co₈₀Pt₂₀ layers by using a fully relativistic noncollinear first principles method, which is suitable for simulating the impact of domain walls on electrical transport. Assuming a perpendicular alignment between the magnetic moments in the domain walls and the electric current direction (see Fig. 2), we are able to directly calculate the magnetoresistance due to the domain walls without having contributions from the AMR involved. Early magneto-optical experiments of Zepper *et al.*¹⁷ showed that the magnetic orientation in the Co-Pt-layered system depends on the thickness of the Co layer. The magnetic moments in ultrathin Co films prefer an orientation perpendicular to the planes, turning to in-plane orientation with increasing thickness of the FM film due to the magnetocrystalline anisotropy. In order to take into account the orientation dependence of the magnetic moments, we have studied two different configurations. In the first case, we consider a domain wall of Bloch type, which has been oriented in the plane of layers with the current perpendicular to the plane (CPP) geometry [see Fig. 2(a)]. In order to allow out-of-plane orientation of the magnetic moments in thin Co films, in the second configuration we consider the magnetic

moments oriented in the \hat{y} - \hat{z} plane and current flowing in the \hat{x} direction, i.e., the CIP geometry [compare Fig. 2(b)]. In general, the width of domain walls depends on the magneto-crystalline anisotropy of the material with decreasing width for increasing anisotropy energy.¹⁸ Co and $\text{Co}_x\text{Pt}_{1-x}$ ($0.72 \leq x \leq 0.8$) possess a large magnetocrystalline anisotropy and the width of the domain walls in these systems is rather small, i.e., on the order of 10 nm in Co, a range that is accessible to *ab initio* methods.

The large magnetocrystalline anisotropy makes Co and CoPt interesting systems for *ab initio* investigations because domain walls in hard magnetic materials are rather small compared to the case of soft magnetic materials such as Fe. Although there is no doubt that domain walls contribute to the magnetoresistance of multilayers or nanowires, there is not much known about the DWMR on the atomic scale, especially in the case of very thin magnetic layers. Experimental data are often compared to the model of Levy and Zhang,¹² which allows us to discuss the experimental results and which predicts that the DWMR decreases with $1/L^2$, where L is the width of the domain wall.

This paper focuses on an analysis of the different contributions to the magnetoresistance in Co or Co-Pt films. All investigated films are grown in the fcc(001) direction, which is in accordance with the experimental condition of Leven¹⁹ for Co-Pt nanowires with a fcc crystal structure, and the experimental setup of Dumpich²⁰ for Co nanowires being partially fcc. The dependence of the magnetoresistance on the thickness of the FM layer will be discussed as well as the geometry (CIP or CPP). Here, all systems are two-dimensional translational invariant, i.e., periodic boundary conditions are implied only for the in-plane directions.²¹ This allows us to address the issue of the top electrodes, which we take as bulk Pt or vacuum, respectively, permitting us to explore how far the simplifying assumption of a semi-infinite Pt bulk system on top of the film influences the magnetoresistance of the system.

II. MODEL AND COMPUTATIONAL METHODS

As mentioned before, a relativistic spin-polarized version of the screened Korringa–Kohn–Rostoker method has been employed in the electronic structure calculations.²² The exchange correlation energy is described in the local density approximation by adapting the formulation of Vosko *et al.*²³ Alloy formation has been included within the coherent potential approximation.

The investigated Co and Co-Pt films are embedded between two semi-infinite systems. We use fcc Pt(001) as the substrate and electron source and optionally fcc Pt(001) or vacuum on top of the FM film (see Fig. 1). Hence, periodic boundary conditions apply only in the film plane (\hat{x} - \hat{y} plane), which leads, in contrast to experiment, to an infinite cross section area.

Since the semi-infinite systems are not included in the self-consistent electronic structure calculation of the film, a particular number of extra Pt and/or vacuum layers have been added to the FM film,

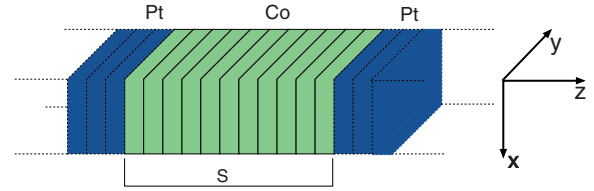


FIG. 1. (Color online) Schematic of the multilayer structure. Periodic boundary conditions have been applied in the \hat{x} - \hat{y} direction. In the \hat{z} direction, the actual multilayer is covered by two semi-infinite Pt(001) systems. S describes the thickness of the multilayer, i.e., the number of atomic layers in the \hat{z} direction.

$$\begin{aligned} & \text{Pt(001)}/\text{Pt}_j/\text{FM}_m/\text{Pt}_k/\text{Pt(001)} \\ & \text{or Pt(001)}/\text{Pt}_j/\text{FM}_m/\text{Pt}_k/\text{Vac}/\text{vacuum}, \\ & 2 \leq m \leq 60, \end{aligned}$$

where the number of buffer layers (j, k) is 9–11 in the case of Pt and $3 \leq l \leq 5$ in the vacuum case. The total number of layers corresponds to $S = m + j + k (+l)$. No lattice relaxations have been taken into account; instead, the bulk lattice constant of fcc Pt, $a = 3.924 \text{ \AA}$, is used in all calculations.

A. Description of domain walls within *ab initio* methods

The investigated systems consist of S layers composed of two magnetic domains of width $S/2$ if m is even. In the case of S being odd, the two domains have the width $(S+1)/2$ and $(S-1)/2$. Assuming that the magnetic moments of two domains are aligned antiparallel, a direct flip of the magnetic orientation at the interface will be energetically unfavorable. From experiment, it is known that this problem is usually overcome by the formation of a domain wall at the interface,¹⁸ which minimizes the magnetostatic energy. This was also confirmed by previous *ab initio* calculations for Co and Co-Pt alloys.²⁴ In the case of a 90 \AA thick $\text{Co}_{80}\text{Pt}_{20}$ film, the energy difference between a direct flip of the magnetic moment and a domain wall configuration amounts to 7 mRy/layer (see Ref. 25).

For all systems presented here, the layers are arranged parallel to the \hat{x} - \hat{y} plane. Starting from a collinear magnetic configuration, in which the two domains of width m_1 and m_2 are aligned in parallel,

$$C_0 = \underbrace{\{\hat{\mathbf{n}}_0, \dots, \hat{\mathbf{n}}_0\}}_{m_1}, \underbrace{\{\hat{\mathbf{n}}_0, \dots, \hat{\mathbf{n}}_0\}}_{m_2}, \quad (1)$$

with $S = m_1 + m_2$, we define the domain wall configuration as follows:

$$C_L = \underbrace{\{\hat{\mathbf{n}}_0, \dots, \hat{\mathbf{n}}_0\}}_{m'_1}, \underbrace{\{\hat{\mathbf{n}}_1^\alpha, \dots, \hat{\mathbf{n}}_L^\alpha\}}_L, \underbrace{\{-\hat{\mathbf{n}}_0, \dots, -\hat{\mathbf{n}}_0\}}_{m'_2}, \quad (2)$$

leading to $S = m'_1 + m'_2 + L = m_1 + m_2$. The vectors $\hat{\mathbf{n}}_p^\alpha$ and $\hat{\mathbf{n}}_0$ represent the orientation of the magnetic field in the layers. By taking into account that the magnetic orientation in Co-Pt-layered systems strongly depends on the thickness of the FM Co layer, we have investigated two different types of magnetic configurations. An in-plane orientation for which

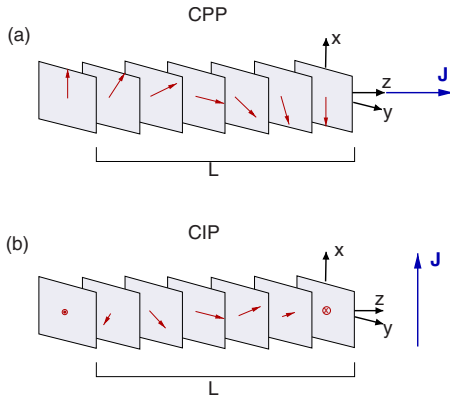


FIG. 2. (Color online) Sketch of the different domain wall geometries. (a) The Bloch domain wall marked by arrows. The magnetic moments of each plane are oriented parallel to the \hat{x} - \hat{y} plane, where the current J is perpendicularly oriented to the plane of layers. This is denoted by CPP. (b) The magnetic moments of the Néel domain wall are lying in plane parallel to the \hat{y} - \hat{z} plane and the current flows parallel to the plane of layers in the \hat{x} direction, which is denoted by CIP.

\hat{n}_0 in Eqs. (1) and (2) is oriented parallel to the \hat{x} axis, which is preferred by thick Co layers, and a second configuration, which is realized in thin Co layers with $\hat{n}_0 \parallel \hat{z}$. The domain walls are oriented with respect to these configurations parallel to the \hat{x} - \hat{y} plane in the first case and in the \hat{y} - \hat{z} plane in the latter one (cf. Fig. 2). In the domain walls, the magnetic orientation changes from layer to layer by a constant angle. In spherical coordinates, the magnetic orientation \hat{n}_p^α of a layer p is given by

$$\hat{x}\text{-}\hat{y}\text{-wall: } \hat{n}_p^\varphi = \left[\vartheta = \frac{\pi}{2}, \varphi(p) \right],$$

$$\hat{y}\text{-}\hat{z}\text{-wall: } \hat{n}_p^\vartheta = \left[\vartheta(p), \varphi = \frac{\pi}{2} \right],$$

$$\varphi(p) = \vartheta(p) = p \frac{\pi}{L}, \quad p = \{1, \dots, L\},$$

which is different from the arctanlike shape that is usually used in the phenomenological Ginzburg–Landau theory.²⁶ It has been shown that the arctan profile is the exact micromagnetic solution if the system size is large compared to the domain wall width. However, in the limit that L and the system size are comparable, the profile changes into a coslike shape.²⁷ Furthermore, Schwitalla *et al.*²⁸ also showed that such simplified profiles are suitable in the *ab initio* description of Bloch walls in ferromagnets. For a detailed discussion of how to calculate Bloch walls from first principles and a comparison to the results from the Ginzburg–Landau theory, we refer to their paper.²⁸ Since the width of the largest investigated domain wall in our work barely reaches the experimentally determined width, we have used the cos profile in all our calculations. For energetic details of domain wall formation for Pt/Co/Pt and Pt/CoPt/Pt, see Ref. 25.

Here, we limit the discussion to the magnetoresistance in alike systems.

B. Magnetoresistance

The AMR is defined as the difference of resistances ρ_{\parallel} and ρ_{\perp} , where \parallel and \perp refer to the relative orientation of current and magnetic moments,

$$R_{\text{AMR}} = \frac{\rho_{\parallel} - \rho_{\perp}}{\rho_{\parallel}}. \quad (3)$$

The magnetoresistance caused by a domain wall in a FM layer can be described by

$$R_{\text{DWMR}} = \frac{\rho_L - \rho_0}{\rho_0}, \quad (4)$$

where ρ_0 is the resistance of the FM reference state C_0 [see Eq. (1)] and ρ_L is the resistance of the same system, but for the domain wall configuration C_L [cf. Eq. (2)].

We make use of the Kubo–Greenwood equation, which provides the diagonal elements of the conductivity tensor $\sigma_{\mu\mu}$ ($\mu \in \{x, y, z\}$), in order to investigate the different magnetoresistive contributions to Pt/Co/Pt and Pt/Co₈₀Pt₂₀/Pt trilayers.^{21,29} The elements of the conductivity tensor depend on the size of the system S , the magnetic configuration C , and the imaginary part δ of the complex Fermi energy $E_F = \varepsilon_F + \delta$. The use of the complex energy is favorable when performing k -space integration and handling surface Green's functions. For given C and S , the actual sheet resistance is determined in the limit $\delta \rightarrow 0$. This is achieved by calculating the elements of the conductivity for finite values of δ and numerical continuation to the real axis. Since the AMR and DWMR are relatively small quantities, the integrals over the surface Brillouin zone have to be calculated with high accuracy. The number of k points used in the irreducible part of the Brillouin zone amounts to 21.000 k_{\parallel} points for the Pt covered systems and to 45.150 k_{\parallel} points in the case of vacuum.

For the CPP geometry (current parallel to the surface normal), the Kubo–Greenwood equation can be used to calculate the conductivity in the steady state.³⁰ The resistance is then obtained by summing over all contributions,

$$\sum_{q=1}^S \rho_{pq}(S, C) \sigma_{qr}(S, C) = \delta_{pr},$$

where $\rho_{pq}(S, C)$ corresponds to the resistance related to the current in layer p and the electric field in layer q . However, $\rho_{pq}(S, C)$ depends on the thickness of the film S , the imaginary part δ of the complex Fermi energy, and the magnetic configuration C . The actual sheet resistance is obtained for $\delta \rightarrow 0$ and by summation over the contributions from all layers,

$$r(S, C) = \lim_{\delta \rightarrow 0} r(S, C, \delta) = \lim_{\delta \rightarrow 0} \sum_{p,q=1}^S \rho_{pq}(S, C, \delta). \quad (5)$$

Then, the AMR can be determined from Eq. (3) by replacing ρ_{\perp} by $r(S, C_0(\hat{n}_0 \parallel \hat{x}))$ and ρ_{\parallel} by $r(S, C'_0(\hat{n}_0 \parallel \hat{z}))$, respec-

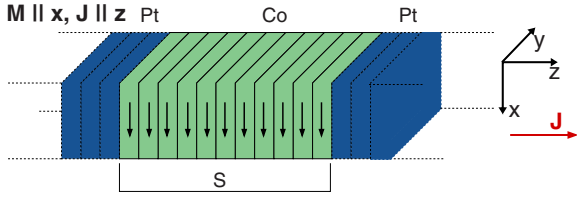


FIG. 3. (Color online) Configuration for the calculation of ρ_{\perp} of the CPP AMR. The current is parallel to the \hat{z} direction and the magnetization is oriented in plane.

tively, where C'_0 corresponds to the collinear magnetic configuration with magnetic moments aligned parallel to the CPP current (see Fig. 3).

In the case of the CIP geometry, the calculation of the conductivity is straightforward. The conductivity directly follows from the Kubo–Greenwood equation and yields $\sigma_{\mu\mu}(S, C_L)$ with $\mu \in \{x, y\}$. The resistivity is then given by

$$\rho_{\mu\mu}(S, C) = \lim_{\delta \rightarrow 0} \{\sigma_{\mu\mu}(S, C, \delta)\}^{-1}, \quad (6)$$

and the CIP AMR is determined by¹⁶

$$R_{\text{AMR}} = \frac{\rho_{xx}(S, C_0) - \rho_{yy}(S, C_0)}{\rho_{xx}(S, C_0)}. \quad (7)$$

Here, the current direction changes between ρ_{\parallel} and ρ_{\perp} , whereas the magnetization direction is kept constant. This is different from the experimental setup, in which the current direction is fixed and the magnetization rotates. However, the AMR depends only on the relative orientation between the two quantities and the results are independent of whether the current or the magnetization direction is changed. We have also investigated the AMR by using a slightly different definition, in which we rotate the magnetic field instead of the current (see Fig. 4),

$$R_{\text{AMR}} = \frac{\rho_{xx}(S, C_0) - \rho_{xx}(S, C'_0(\hat{\mathbf{n}}_0 \parallel \hat{\mathbf{z}}))}{\rho_{xx}(S, C_0)}. \quad (8)$$

When we replace the collinear magnetic configurations C_0 and C'_0 by a noncollinear configuration C_L , as defined in Eq. (2), one obtains the dependence of the magnetoresistance on the relative orientation of current and magnetic configuration. Within our nomenclature, the DWMR then has the following form:

$$\text{CPP: } R_{\text{DWMR}}^{\perp} = \frac{r(S, C_L) - r(S, C_0)}{r(S, C_0)}, \quad (9)$$

$$\text{CIP: } R_{\text{DWMR}}^{\parallel} = \frac{\rho_{xx}(S, C_L) - \rho_{xx}(S, C_0)}{\rho_{xx}(S, C_0)}. \quad (10)$$

where \parallel and \perp correspond to the current direction in plane or perpendicular to the planes, respectively. Now, the conductivity as described in the Kubo–Greenwood formalism contains vertex corrections. Here, only vertex corrections have been included, which arise from the layer dependence of the electric field by the inverting Ohm's law $j = \sigma E$ to $E = \int \rho(z, z') dz'$; for a detailed discussion, we refer the reader to Ref. 31. The error, which is made by neglecting further

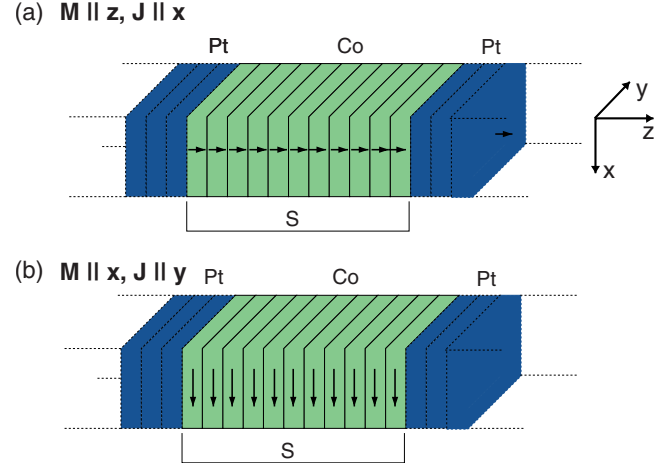


FIG. 4. (Color online) Schematic of the magnetic configurations used in CIP calculations for ρ_{\perp} . (a) The current flows parallel to the \hat{x} direction and the magnetic moments for ρ_{\parallel} are oriented in the same direction. For ρ_{\perp} , the magnetization is aligned parallel to the \hat{z} direction. (b) Here, the current direction is changed between ρ_{\parallel} ($J \parallel \hat{x}$) and ρ_{\perp} ($J \parallel \hat{y}$). In experiment only, the direction of the magnetization can be changed, but for the AMR, only the relative orientation between current and magnetization plays a role.

vertex corrections, is discussed by Tsymbal and Pettifor.³² They investigated the influence of vertex corrections on the conductivity of Co/Cu and Fe/Cr multilayers and concluded that the changes in the conductivity due to vertex corrections is always smaller than 1% (see also Ref. 33).

III. RESULTS AND DISCUSSION

A. Anisotropic magnetoresistance

1. Pt/Co/Pt(001)

The AMR can be regarded as a measure of the relative orientation dependence of the current and magnetic field in a FM system, including the two extreme cases for which the two quantities are aligned parallel or perpendicular to each other. In Co and Co-Pt nanowires, the AMR was reported to be about 1%.²⁰ However, the absolute value of the AMR is related in addition to the geometry of the sample. Furthermore, in theory we can apply the current parallel and perpendicular to the plane of layers, whereas experimentally, only one geometry is used; for example, only the CPP geometry is used in nanopillars. Experimental studies are often restricted to a certain range of film thicknesses, whereas a systematic variation of the film thickness can easily be done within our theoretical approach. However, the variation in the film thickness is restricted by the computational effort, which is relatively large due to the high accuracy needed for the k -point integration (cf. Sec. II). The investigated systems comprise the range of interest to studies related to the determination of transport properties of layered structures, such as Hall-effect measurements in nanopillars,³⁴ investigations of the magnetoresistance of thin wires,¹⁹ and the influence of magnetocrystalline anisotropy in multilayers.¹⁷

The AMRs of (001)-oriented Pt/Co/Pt systems as obtained from the Kubo–Greenwood approach are plotted in Fig. 5.

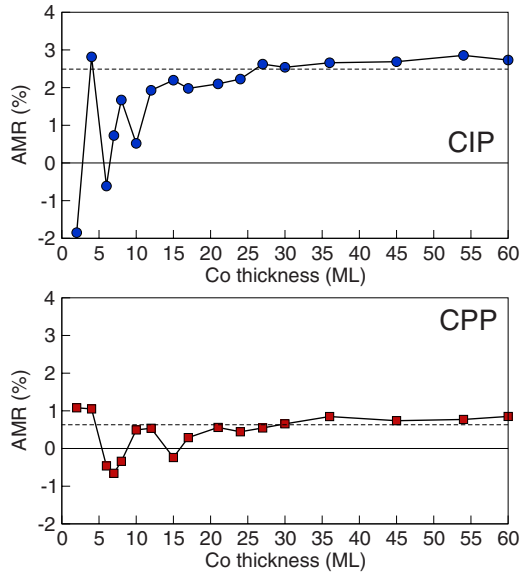


FIG. 5. (Color online) Dependence of the AMR of $\text{Pt}/\text{Co}_m/\text{Pt}(001)$ trilayer systems for the CIP (top) and CPP (bottom) geometries on the thickness m of the Co film in monolayers. The dashed lines mark the limit for large m , i.e., thicknesses of the Co films larger than 30 Å.

The results are given for both symmetries: CIP and CPP. In the case of an in-plane current, two possibilities defining ρ_{\perp} exist [see Eq. (3)]. If we assume that the current direction is aligned parallel to the \hat{x} direction, the magnetic moments can be oriented either parallel to the \hat{y} or to the \hat{z} direction, which defines the transverse or perpendicular AMR, respectively. In the present work, we mainly focus on the transverse AMR with in-plane magnetic orientations because out-of-plane magnetization has only been observed for systems with very thin Co layers.³⁵ For Co film thicknesses of 23.6 Å or larger, the average value of the transverse AMR amounts to, in average, 2.4%. For thinner Co films, the AMR shows distinct oscillations with the Co thickness. This type of oscillations is related to the geometry and seems to be similar to the oscillations observed in supercell calculations due to quantum confinement.^{36,37}

In the case of CPP geometry, the AMR is considerably smaller, being on the order of 0.63% ($m \geq 17$ monolayers). The CPP AMR results are close to the experimental values of 0.7%–0.8% for bulk Co and 1% for Co films and wires.^{38,39} The fact that the CIP AMR is large compared to the CPP one and the experimental values seems to be related to the underlying lattice structure. As mentioned in Sec. II, lattice relaxation effects are not included, and for the lattice spacing the Pt lattice constant was used. Calculations for a bulklike Co system support the assumption that the overestimation of the CIP AMR is related to the underlying bulk system because a (001)-oriented Co layer ($m=48$) with Co contacts (lattice constant $a=3.53$ Å) give a transverse AMR value of 0.74%, which is in good agreement with the experimental results.¹⁰ The origin of the negative AMR values will be addressed below in conjunction with the discussion of the influence of the surface Pt layer.

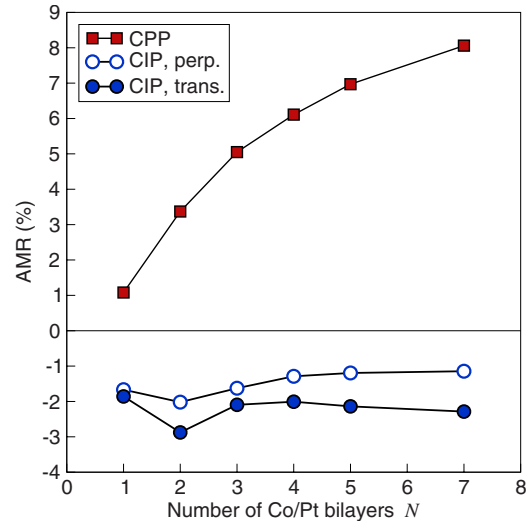


FIG. 6. (Color online) CPP (squares) and CIP (circles) AMR of $\text{Pt}/(\text{Co}_2\text{Pt}_7)_N/\text{Pt}$ ($1 \leq N \leq 7$) multilayers. In the CIP case, two different configurations have been used [see Eqs. (7) and (8) and Fig. 4]. The filled circles mark the in plane orientation and the open circles denote the out-of-plane orientation of the magnetic moments.

2. Co-Pt multilayer

Nanopillars and thin films used in realistic devices are commonly built of multilayers or alloys instead of pure FM metals.⁴⁰ Therefore, we address now the issue in how far the MR changes when we replace the Co film by a Co-Pt multilayer. The investigated multilayers consist of N (Co_2Pt_7) ($1 \leq N \leq 7$) bilayers with $j=11$ and $j=4$ Pt buffer layers on the top and bottom of the actual multilayer (cf. Sec. II), such that $N=1$ corresponds to the $\text{Pt}_{11}/\text{Co}_2/\text{Pt}_{11}$ trilayer (Fig. 6).

In contrast to the previously discussed $\text{Pt}/\text{Co}_n/\text{Pt}$ trilayers, no thickness dependent oscillations are observed in the AMR. Calculations for the CIP geometry yield negative AMR values, which are constant for $N > 2$. The transverse AMR is about -2% , whereas the perpendicular AMR amounts to -1.3% . The differences between the two values are related to numerical errors due to the fitting procedure. The negative sign seems to be an artifact of the semi-infinite Pt system on top of the multilayer (see the discussion in Sec. III A 3). The CPP AMR increases with the number N of bilayers being about 8% for $N \geq 7$ and monotonically increases with the number of bilayers and in a logarithmiclike manner. To our knowledge, such large AMR values have not been experimentally observed so far for Co-Pt films and may result from the use of equilibrium Green's functions and, hence, the neglect of spin-accumulation effects at the interfaces. Obviously, the differences between the CIP and the CPP AMRs for small N are related to the results obtained for a single trilayer ($N=1$, $m=2$), where the CIP AMR is also negative in the case of $m=2$, i.e., the behavior of the AMR in Co-Pt multilayers is essentially determined by the number of Co layers per bilayer and less by the total thickness of the Co-Pt film.

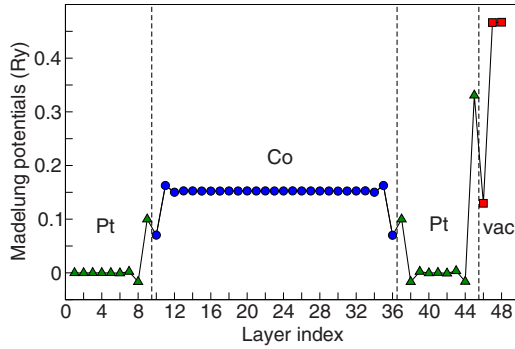


FIG. 7. (Color online) Layer-resolved Madelung potentials of Pt(001)/Pt₉/Co₂₇/Pt₉/Vac₃/Vac. The Pt layers are marked by the triangles, the filled circles correspond to Co, and the vacuum levels are denoted by squares; the vacuum potential level is $E_{\text{vac}} = 0.467$ Ry.

3. Pt/Co/Pt/vacuum

In fact, the assumption of a semi-infinite Pt lead on top of a Co layer is a simplified model of a real metallic contact layer. However, in transport experiments, the top coat is often relatively thin, amounting to 1–2 nm in the case of Co and Co-Pt wires covered by Pt like in Refs. 19 and 38. In order to check whether the negative AMR values obtained for (001)Pt/CoPt(001) are related to the constitution of the top electrode, we recalculated the AMR of the trilayers by replacing the semi-infinite Pt system by a finite Pt top coat consisting of nine Pt layers. In this case, one semi-infinite system is replaced by vacuum (see Sec. II). The influence of the vacuum on the electrostatic Madelung potential is shown in Fig. 7 for the case of Pt(001)/Pt₉/Co₂₇/Pt₉/vac₃/vacuum (semi-infinite), wherein three vacuum layers are included in the self-consistently calculated part of the multilayer. The Madelung potentials of the Pt layers tend to the bulk value (zero), whereas the values of the Co layers lie 0.15 Ry higher in energy. Considerable variations in the Madelung energy can only be observed close to the Pt-Co and Pt-vacuum interfaces. However, in both cases, the Madelung potentials very rapidly approach the Co value or the calculated vacuum level of 0.467 Ry. Since charge transfer effects at the metal vacuum interface seem to be very short ranged, we first used a constant vacuum level in the AMR calculations. Except for very thin Co films, the magnitude and the thickness dependences of the AMR are very similar to the previously discussed case of Pt(001)/Co_m/Pt(001) trilayers. For thin Co layers, the AMR values are smaller compared to those for the previous case without vacuum; in the case of $m=2$, we obtain $R = -0.37\%$ instead of -5.38% .

By taking into account the exact electrostatic potential of the vacuum buffer layers, we obtain drastic changes for the AMR, as shown in Fig. 8. The strong oscillations observed for thin Co films have vanished and all of the AMR values are positive. However, the most distinct differences occur for larger film thicknesses. The AMR values are reduced by a factor of 2, now being $\sim 1.1\%$ (averaging results for $m > 10$), which is in very good agreement with the experimental results. As mentioned in Sec. II, the resistivities have been calculated in the complex energy plane, which means that a

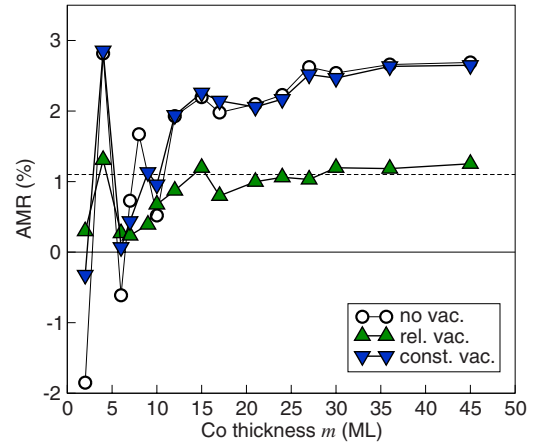


FIG. 8. (Color online) Calculated AMR of the Pt/Co_m/Pt/Vac system as a function of the thickness of the Co film. The current is oriented parallel to the plane of layers (CIP). Results are given for the constant vacuum level (down triangles) and self-consistently treated vacuum (up triangles) (see text for details). For comparison, the corresponding results for trilayers without vacuum are also shown (circles). The dashed line corresponds to the average AMR in case of a self-consistent treatment of the vacuum buffer layers for $m > 10$.

finite imaginary part is attributed to the Fermi energy. In order to obtain the actual resistivities, we have to extract the $\delta \rightarrow 0$ value,³³ which has been done by a linear fit to the δ -dependent resistivities. The error in this fitting procedure is about 2%–6% for CIP conductivities. The actual magnitude depends on the type of the system, i.e., the vacuum capped systems give somewhat larger errors compared to the case of Pt covered trilayers. In the case of vacuum being included in the self-consistently calculated part of the super cell, a linear behavior could only be achieved for $\delta \geq 2$ mRy. In the CPP geometry, the errors are below 0.5%.

B. Domain wall resistance

Besides the *natural* anisotropic magnetoresistance, which a single domain structure establishes, additional contributions arise in the more interesting case of multidomain structures, such as the domain walls that occur at the interfaces of regions with different magnetic orientations. Here, the magnetoresistance of domain walls in Co and Co₈₀Pt₂₀ alloy films with Pt contacts has been studied by adopting Eq. (4). In order to avoid contributions from the AMR, it has to be ensured that the domain wall is always oriented perpendicular to the current. Assuming that the current \mathbf{J} is aligned parallel to the surface normal (\hat{z} direction) [see Fig. 2(a)], the magnetic reference configuration C_0 and the domain walls are oriented parallel to the plane of layers with $C_0 = \{\hat{x}, \dots, \hat{x}\}$ [Eq. (1)]. However, ultrathin (< 5 Å) Co films between Pt layers possess a perpendicular magnetocrystalline anisotropy at surfaces and interfaces, which provokes an out-of-plane orientation of the magnetic moments.³⁵ Therefore, we consider a second configuration with an out-of-plane orientation of the domain wall with the magnetic orientation rotating in the \hat{y} - \hat{z} -plane and the \mathbf{J} orientation

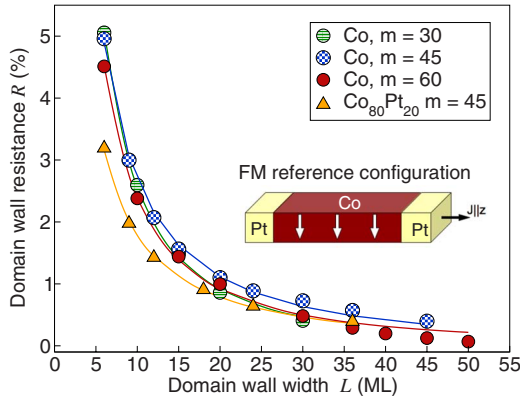


FIG. 9. (Color online) Calculated domain wall magnetoresistance for the in-plane orientation of the magnetic moments. The current flows perpendicular to the magnetic moments, i.e., parallel to the surface normal. The inset shows the collinear magnetic reference configuration.

parallel to the \hat{x} direction (CIP) [cf. Fig. 2(b)]. The reference configuration corresponds to $C_0 = \{\hat{z}, \dots, \hat{z}\}$. The widths of the FM layers used to study the DWMR are $m=30$, 45, and 60 layers of Co. In the case of $\text{Co}_{80}\text{Pt}_{20}$, only $m=45$ has been taken into consideration. The FM layer is assumed to consist of two magnetic domains and a domain wall in between [see Eq. (2)]. The domain wall widths range from six monolayers to the full size of the FM layer. In the case of extremely tiny walls with widths on the order of 1 nm, which are under normal conditions not observed in nature, the DWMR values are uncommonly high, being approximately 5% for Pt/Co/Pt in the CPP geometry (Fig. 9) and even 17%–18% in the CIP geometry (Fig. 10). The CPP DWMR of $\text{Co}_{80}\text{Pt}_{20}$ alloy films is considerably smaller, being $<3.5\%$ for $m=6$. For the largest investigated systems, we are already in the range of realistic domain wall widths of Co systems.¹⁸ The DWMR is then about 0.5% (CPP) and 2.8%–3.5% (CIP).

As expected, the DWMR diminishes with increasing width of the domain wall. Levy and Zhang¹² claimed that this decrease should be on the order of $1/L^2$, where L is the

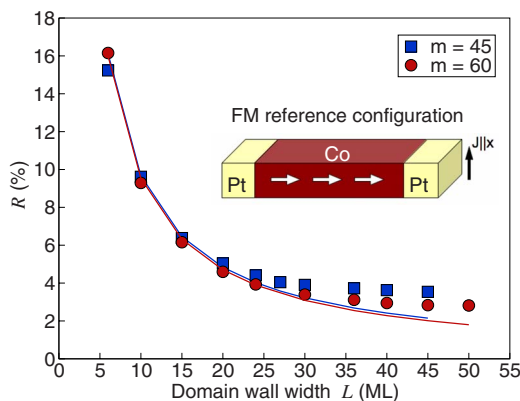


FIG. 10. (Color online) Domain wall magnetoresistance for an orientation of the magnetic moments in the \hat{y} - \hat{z} plane. The current is applied in the \hat{x} direction, i.e., perpendicular to the orientation of the magnetic moments. The inset shows the collinear magnetic reference configuration.

TABLE I. Fit parameters used for a and L_{\min} in Eq. (11).

System	a	L_{\min}
Co, $S=60$	1.67	20.67
Co, $S=45$	0.90	37.80
Co, $S=30$	2.79	15.23
$\text{Co}_{80}\text{Pt}_{20}$, $S=45$	0.34	61.35

width of the domain wall. Within the present *ab initio* investigations we are able to verify this model at least for large domain wall widths. Since their model was made for macroscopic systems, it could not be implied that it would also hold for relatively small domain wall widths in which the magnetization changes relatively abruptly. Our calculations show that systems with extremely tiny domain walls show deviations from the expected $1/L^2$ behavior. In these cases, the DWMR seems to linearly decrease with the width of the domain wall. In order to determine the onset of the $1/L^2$ behavior, we fit our results to the following expression:

$$R_{\text{DW}}(L) = \frac{a}{\left(\frac{L}{L_{\min}}\right)^2 + \left(\frac{L}{L_{\min}}\right)}, \quad (11)$$

where L_{\min} determines the minimum width of the domain wall, which is needed to observe a quadratic, $1/L^2$, decay. According to Eq. (11), the DWMR in systems with $L < L_{\min}$ is assumed to linearly decay with the domain wall width. The prefactor a in Eq. (11) can be viewed as a measure of the absolute size of the DWMR; the larger a is, the larger the DWMR is. In the case of out-of-plane currents, the calculated values fit well this expression (see Fig. 9). The onset of the expected $1/L^2$ behavior depends on the actual structure of the ferromagnet and the width of the FM layer. In systems with pure Co films, L_{\min} ranges from 15.23 to 37.8 monolayers, whereas in the case of the $\text{Co}_{80}\text{Pt}_{20}$ alloy, L_{\min} is twice as large as in the Co case (see Table I). However, small deviations from the assumed shape [Eq. (11)] are observed if L and the width of the FM layer m are of the same size. These deviations can be traced back to the fact that in the considered systems, the domain wall and the FM domains are the same and the DWMR is already quite small, which makes the calculation slightly more faulty than for smaller L . Apart from this small discrepancies, the calculated DWMR follows the predictions from Levy and Zhang¹² for domain wall widths larger than L_{\min} .

Whether the prediction of $1/L^2$ decay also holds for domain walls oriented in the \hat{y} - \hat{z} plane and in-plane currents has been studied for Co films with $m=45$ and 60. As mentioned above, the DWMR strongly decreases with increasing width of the domain wall, whereby no significant dependence on the wall width is observed. In contrast to the previously discussed CPP case, the calculated DWMR for the largest domain walls exceeds the expected value by a factor of 3, being 2.8% in the case of $m=50$ monolayers. In consideration of the previous discussion concerning the influence of the top electrode on the magnetoresistance, the large

DWMR is not surprising. The slight overestimation can be ascribed to the choice of the top contact, which is bulk Pt instead of vacuum.

However, as in the previous case a linear slope is observed in the limit of small domain walls, but with increasing width of the domain wall, the calculated magnetoresistance deviates from the predicted $1/L^2$ behavior. If the domain wall width becomes larger than 7 nm, the slope of the DWMR is more or less zero; i.e., in this case, the DWMR seems not to obey the prediction by Levy and Zhang.¹²

IV. CONCLUSIONS

We have studied the magnetoresistance of Co and Co₈₀Pt₂₀ films with Pt contacts by using a first principles scattering approach, namely, the SKKR method and the Kubo–Greenwood formalism, in order to determine the conductivity and the magnetoresistances of these systems. All of the calculations have been fully relativistically performed to allow for the calculation of the AMR, which depends on spin-orbit coupling. The influence of domain walls on the magnetoresistance just as the AMR have been investigated for FM layers with different widths and orientations. For the current perpendicular to the plane geometry (CPP), the AMR compares well to the experimental findings of $\approx 0.5\%–1\%$.¹⁸ In the case of the in-plane geometry (CIP), the results depend on the structure of the top contact, i.e., a semi-infinite Pt bulk system gives slightly higher AMR values as compared to systems with thin Pt top coats and semi-infinite vacuum. The magnetoresistance of the latter one is in a good agreement with experimental results.

The influence of domain walls on the magnetoresistance has been investigated for selected widths of the FM layer

ranging from 45 to 60 monolayers (8.83–11.77 nm) in view of the width dependence of the domain wall magnetoresistance. We have performed calculations for two different symmetries, namely, domain walls with magnetic orientation parallel to the plane of layers (\hat{x} - \hat{y} plane) and walls being oriented in the \hat{y} - \hat{z} plane. The current was always perpendicularly oriented to the domain walls. In the case of in-plane domain walls, the DWMR rapidly decreases with increasing width of the domain wall L . For small domain wall widths, the DWMR decays with $1/L$, which gives way to a $1/L^2$ behavior for larger wall widths. The transition from linear to quadratic decay depends on the FM material, which is Co or Co₈₀Pt₂₀ here, and the thickness of the FM layer. In the case of pure Co, the onset of the $1/L^2$ behavior can already be observed for $L \approx 30–74$ Å, whereas in Co₈₀Pt₂₀, the transition from linear to quadratic decay takes place for larger widths of the order of $L \approx 120$ Å. In the case of \hat{y} - \hat{z} -oriented domain walls, we obtain also a linear decay for small domain wall widths, but no $1/L^2$ behavior could be observed. For the latter geometry, the DWMR mainly becomes constant for large wall widths. However, the magnetic configuration chosen here is favorable for very thin Co films in Pt/Co/Pt trilayers;³⁵ therefore, thicker Co films would naturally not provide domains oriented parallel to the surface normal. In how far the bulklike Pt top electrode is also responsible for the constant slope could not be decided and has to be studied in future work.

ACKNOWLEDGMENTS

H.C.H. would like to thank A. Hucht for fruitful discussions. This work was supported by the Deutsche Forschungsgemeinschaft through Grant No. SFB 491 *Magnetic Heterostructures: Spinstructure and Spintransport*.

¹A. Fert, P. Grünberg, A. Barthélémy, F. Petroff, and W. Zinn, *J. Magn. Magn. Mater.* **140-144**, 1 (1995).

²P. Grünberg, *J. Magn. Magn. Mater.* **226-230**, 1688 (2001).

³*Spin Dependent Transport in Magnetic Nanostructures*, edited by S. Maekawa and T. Shinjo (Taylor & Francis, London, 2002).

⁴J. Mathon, in *Spin-Electronics*, Lecture Notes in Physics Vol. 569, edited by M. Ziese and M. Thornton (Springer, Berlin, 2001), p. 71.

⁵J. Kudrnovsky, V. Drchal, I. Turek, P. Weinberger, and P. Bruno, *Comput. Mater. Sci.* **25**, 584 (2002).

⁶H. C. Herper, P. Entel, L. Szunyogh, and P. Weinberger, *Magnetolectronics—Novel Magnetic Phenomena in Nanostructures*, MRS Symposia Proceedings No. 746 (Materials Research Society, Pittsburgh, 2003), p. 101.

⁷G. R. Taylor, A. Isin, and R. V. Coleman, *Phys. Rev.* **165**, 621 (1968).

⁸J. F. Gregg, W. Allen, K. Ounadjela, M. Viret, M. Hehn, S. M. Thompson, and J. M. D. Coey, *Phys. Rev. Lett.* **77**, 1580 (1996).

⁹J. L. Prieto, M. G. Blamire, and J. E. Evetts, *Phys. Rev. Lett.* **90**, 027201 (2003).

¹⁰C. Hassel, M. Brands, F. Y. Lo, A. D. Wieck, and G. Dumpich,

Phys. Rev. Lett. **97**, 226805 (2006).

¹¹U. Nowak, J. Heimele, T. Kleinfeld, and D. Weller, *Phys. Rev. B* **56**, 8143 (1997).

¹²P. M. Levy and S. Zhang, *Phys. Rev. Lett.* **79**, 5110 (1997).

¹³L. Berger, *Phys. Rev. B* **73**, 014407 (2006).

¹⁴J. B. van Hoof, K. M. Schep, P. Kelly, and G. E. Bauer, *J. Magn. Magn. Mater.* **177-181**, 188 (1998).

¹⁵B. Y. Yavorsky, I. Mertig, A. Ya. Perlov, A. N. Yaresko, and V. N. Antonov, *Phys. Rev. B* **66**, 174422 (2002).

¹⁶S. Gallego, P. Weinberger, L. Szunyogh, P. M. Levy, and C. Sommers, *Phys. Rev. B* **68**, 054406 (2003).

¹⁷W. B. Zeper, F. J. A. M. Greidanus, P. F. Garcia, and C. R. Fincher, *J. Appl. Phys.* **65**, 4971 (1989).

¹⁸A. D. Kent, U. Rüdiger, and S. Parkin, *J. Phys.: Condens. Matter* **13**, R461 (2001).

¹⁹B. Leven, U. Nowak, and G. Dumpich, *Europhys. Lett.* **70**, 803 (2005).

²⁰G. Dumpich, T. Krome, and B. Hausmanns, *J. Magn. Magn. Mater.* **248**, 241 (2002).

²¹P. Weinberger, P. M. Levy, J. Banhart, L. Szunyogh, and B. Újfalussy, *J. Phys.: Condens. Matter* **8**, 7677 (1996).

²²P. Weinberger and L. Szunyogh, *Comput. Mater. Sci.* **17**, 414

- (2000).
- ²³S. H. Vosko, L. Wilk, and M. Nusair, *Can. J. Phys.* **58**, 1200 (1980).
- ²⁴H. C. Herper, *Advances in Solid State Physics* (Springer, New York, 2008), Vol. 46, p. 269.
- ²⁵H. Herper and P. Entel, *Phase Transitions* **79**, 827 (2006).
- ²⁶A. M. Kosevich, in *Modern Problems in Condensed Matter Science*, edited by V. M. Agranovich and A. Maradudin (North-Holland, Amsterdam, 1986), Vol. 17, p. 595.
- ²⁷N. Kazantseva, R. Wieser, and U. Nowak, *Phys. Rev. Lett.* **94**, 037206 (2005).
- ²⁸J. Schwitalla, B. L. Györfy, and L. Szunyogh, *Phys. Rev. B* **63**, 104423 (2001).
- ²⁹P. Weinberger, *Phys. Rep.* **377**, 281 (2003).
- ³⁰P. M. Levy, *Solid State Physics* (Academic, Cambridge, 1994), Vol. 47.
- ³¹H. Herper, *Phys. Status Solidi B* **243**, 2632 (2006).
- ³²E. Y. Tsybal and D. G. Pettifor, *Phys. Rev. B* **54**, 15314 (1996).
- ³³P. Weinberger, L. Szunyogh, C. Blaas, and C. Sommers, *Phys. Rev. B* **64**, 184429 (2001).
- ³⁴N. Kikuchi, R. Murillo, and J. C. Lodder, *J. Appl. Phys.* **97**, 10J713 (2005).
- ³⁵A. Aziz, S. Bending, H. Roberts, S. Crampin, P. J. Heard, and C. Marrows, *J. Appl. Phys.* **99**, 08C504 (2006).
- ³⁶W. H. Butler, X.-G. Zhang, D. M. C. Nicholson, T. C. Schulthess, and J. M. MacLaren, *Phys. Rev. Lett.* **76**, 3216 (1996).
- ³⁷P. Zahn, J. Binder, and I. Mertig, *Phys. Rev. B* **72**, 174425 (2005).
- ³⁸M. Brands and G. Dumpich, *J. Phys. D* **38**, 822 (2005).
- ³⁹Y. D. Yao, Y. Liou, J. C. A. Huang, S. Liao, C. H. Lee, K. T. Wu, Y. Chen, C. L. Lu, and W. T. Yang, *Chin. J. Phys. (Taipei)* **32**, 340 (1994).
- ⁴⁰H. X. Wei, T. X. Wang, Z. Zeng, X. Q. Zhang, J. Zhao, and X. F. Han, *J. Magn. Magn. Mater.* **303**, e208 (2006).